Research Square

Preprints are preliminary reports that have not undergone peer review.
They should not be considered conclusive, used to inform clinical practice,
or referenced by the media as validated information.

Self-Consistent Field Solution for Anions: Effect of the Removal of Pseudo-Continuum States

Deepak Kumar
Indian Institute of Technology Guwahati
Ashish Kumar Gupta
gupta@iitg.ac.in

Indian Institute of Technology Guwahati

Research Article

Keywords: electronic resonance, complex absorbing potential, variational collapse, pseudo-continuum states

Posted Date: August 14th, 2026

DOI: https://doi.org/10.21203/rs.3.rs-10565209/v1

License: This work is licensed under a Creative Commons Attribution 4.0 International License.
Read Full License

Additional Declarations: No competing interests reported.

Self-Consistent Field Solution for Anions: Effect of the Removal of Pseudo-Continuum States

Deepak Kumar[1] and Ashish Kumar Gupta[1*]

[1]Department of Chemistry, Indian Institute of Technology Guwahati, Guwahati, 781039, Assam, India.

*Corresponding author(s). E-mail(s): gupta@iitg.ac.in;

Abstract

This article introduces an innovative solution to prevent variational collapse for metastable anions by removing the sea of non-physical pseudo-continuum states at the SCF stage and implementing it in a non-Hermitian domain, where the lifetime of the electron attached state can be accessed. This SCF solution is achieved in two steps. First, a SCF calculation is performed on the neutral molecule, and the valence antibonding orbital is identified. Next, the extra electron is added to the valence antibonding orbital, and the SCF calculation for anionic species is carried out by modifying the Fock-matrix after removing the pseudo-continuum states present between HOMO and valence antibonding orbital. The resulting SCF solution corresponds to the metastable anion without any variational collapse. Here, Complex absorbing potential (CAP) is implemented at the Hartree-Fock (HF) level, and the solution obtained at the HF level is then used to perform the post-SCF calculation. Identifying pseudo-continuum states to be excluded for the post-SCF calculation becomes straightforward after the valence antibonding orbital is identified. Removal of these pseudo-continuum states does not have a significant effect on the correlation energy. This SCF solution is highly advantageous, as it contains a reduced number of MOs for post-SCF calculations, thereby saving significant computational time.

Keywords: electronic resonance, complex absorbing potential, variational collapse, pseudo-continuum states

1 Introduction

A "resonance" describes an electronically metastable state, that is, a state of a metastable anion that lies energetically above the ground state of the associated neutral molecule. Under experimental conditions, gas-phase electron affinities (EAs) for many molecules are typically negative, indicating the presence of a metastable state that has a finite lifetime. They can decay by losing an electron, a process known as autodetachment, or by fragmenting into a stable anion and a radical, which is called dissociative electron attachment (DEA)[1–7].

The wave function of a metastable state has an oscillating tail that extends to infinity, which requires the use of diffuse functions in the basis set for accurate representation. Conventional self-consistent field (SCF) calculation may converge to the lowest-energy solution, with the excess electron occupying a diffuse molecular orbital present in the basis set. When using a highly diffuse basis set, the SCF solution may lead to the breakdown of the system into a neutral molecule with a free electron. This is known as variational collapse. As a result, this broken SCF solution is unsuitable for studying metastable anions, as it does not accurately represent a true anionic state. Therefore, obtaining a reliable SCF solution is crucial for effectively describing temporary anions or metastable states when calculating energies at post-SCF levels, such as MP2, CCSD, and CI. However, it is not necessary to achieve a reliable SCF solution for the anion if one employs methods like EOM-EA-CCSD[8–10].

A comprehensive discussion on the advanced methods for the studying of metastable states available in various literature articles and reviews. One such method involves the use of non-Hermitian quantum mechanics, which includes complex scaling[11–14], Modified Smooth Exterior Scaling (MSES)[15–17], and complex-absorbing potential (CAP)[18–20]. Another type of method involves the use of bound state calculations, i.e., conventional Hermitian quantum mechanics. This includes artificially binding an extra electron, which can be accomplished by using a compact basis set or introducing a potential wall[21, 22] to capture the electron inside. Additionally, it also includes stabilization methods[23–29] and extrapolation methods[30–36], which are used to describe the metastable states.

During SCF calculations with a heavily diffuse basis set, we encounter a sea of pseudo-continuum states alongside the important localised states. These pseudo-continuum states are responsible for the variational collapse happening in the study of metastable anions. This phenomenon has been thoroughly discussed in various studies. For instance, variational collapse occurs in the case of SO_4^{2-}, where the SCF method generates the lowest-energy wave function for the $SO_4^- + e^-$ system instead of the wave function for the metastable SO_4^{2-}[37]. Similar instances of variational collapse have also been noted in the temporary anionic states of N_2, CO[16, 38, 39], CH_3CN, CH_3NC[40, 41], CH_3SCN, CH_3NCS[41], chloromethanes[42], polyatomic hydrocarbons[2, 43], silane & linear silanes[44, 45], biological anions that may lead to DEA such as uracil[46–48], and various other metastable anions. If these pseudo-continuum states are indeed responsible for variational collapse, and if they can somehow be eliminated from our solution, then variational collapse would not occur in any scenarios, including at the post-SCF level but will also save computational time. An important task to consider is how many states are being removed and the criteria for this decision. All the states that exist between the Highest Occupied Molecular Orbital (HOMO) and the valence antibonding orbital are pseudo-continuum states and are responsible for variational collapse. Therefore, these states can be removed from the calculations. The valence antibonding orbital

represents the actual state that an additional electron will occupy, characterized by a well-defined and localized shape (for example, the $\pi^\star$ antibonding character in the case of C_2H_4). Identifying the valence antibonding orbital is a crucial step in this methodology; if the incorrect valence antibonding orbital is selected, it can lead to significant inaccuracies in the results. The precise identification of the valence antibonding orbital even when using heavily diffuse basis sets is successfully achieved using nuclear charge stabilization method in conjunction with Parametric Equations of Motion (PEM)[50, 51].

Recently, our group has made an effort to provide an SCF solution for metastable anions while avoiding the variational collapse, and the obtained solution can then be used for post-SCF calculations[49]. However, the earlier article[49] was limited to a Hermitian framework, which did not provide information about the lifetime of the electron attached states. This article aims to address variational collapse solutions by removing the pseudo continuum states and implement it in a non-Hermitian domain, where the lifetime of electron attached state can be accessed. Here, CAP is implemented at Hartree-Fock level and the solution obtained at the HF-level is then used to perform the post-SCF calculation. The obtained non-Hermitian SCF solution is used for post-SCF calculation (i.e. Møller–Plesset perturbation theory (MP2)) in this article to improve the accuracy of the results obtained from Hartree-Fock method. Incorporating the CAP into the physical Hamiltonian H effectively damps the outgoing portion of the continuum wave functions contributing to resonance phenomena. As a result, a resonance state is now associated with a single square-integrable eigenfunction of $H(\eta)$. This means that the resonance state can be considered a discrete bound state after the addition of CAP. This article also examines how much the continuum states (i.e., those between HOMO and the valence antibonding orbital) contribute to the correlation energy for neutral molecules. The correlation energy is calculated at MP2 level of theory and it is observed that the impact of the removal of these pseudo-continuum states on the correlation energy is insignificant. Furthermore, this method should be applicable to excited state calculations and core-excited shape or Feshbach resonances. An electron can attach to an existing excited state configuration, resulting in core-excited shape or Feshbach resonances. In these resonances, the configuration includes a vacancy in an inner filled orbital and two electrons in a virtual orbital[47, 52–54]. Utilizing diffuse basis functions poses significant challenges, particularly due to the attached electron in the most diffuse states and also the difficulty in generating core-excited states. However, if there are no pseudo-continuum states in the calculations, both of these issues will be resolved easily.

In this article, we have examined the SCF solution for the $C_2H_4^-$ and $HCHO^-$ anionic species in non-Hermitian domain after removing the pseudo-continuum states. We have also examined the effect on correlation energies after removing the pseudo-continuum states for both the species by performing calculations at MP2 level. The paper is structured with the next section providing the theoretical background for the approach to remove these pseudo-continuum states by modifying the Fock-matrix. Following that, we present and discuss the results. Finally, we draw our conclusions.

2 Theory

2.1 Complex Absorbing Potential

The Complex Absorbing Potential (CAP) was first introduced by Jolicard and Austin and later modified by Riss and Meyer[18–20]. In this method, the Hamiltonian is perturbed by an appropriate potential to create an absorbing boundary condition. In the CAP approach, divergent resonance wave functions are converted into square-integrable wave functions by adding a complex potential, -iηW, to the physical Hamiltonian H_0,

$$H = H_0 - i\eta W \tag{1}$$

where η is a strength parameter and H has linear dependency on it. W is usually introduced only into the exterior region of the system such that it is zero inside the interaction region and has a finite value outside the interaction region, which can be described by the following equations[55],

$$W = \sum_{i=x,y,z} W_i \tag{2}$$

$$W_i = \begin{cases} 0, & |r_i| < r_i^0 \\ (r_i - r_i^0)^2, & |r_i| > r_i^0 \end{cases} \tag{3}$$

where r_i denotes the three Cartesian coordinates ($i = x, y, z$) and r_i^0 represents the CAP box-size parameter.

A complex absorbing potential is incorporated into the system Hamiltonian to make the resonance wavefunction square integrable. However, the artificial introduction of the CAP does perturb the Hamiltonian. The exact resonance eigenvalues and eigenfunctions can be obtained in the limit as ($\eta \to 0$) when using a complete basis set. In practice, for incomplete basis sets, a finite value of the CAP strength parameter (i.e., η) is necessary to accurately determine the resonance energies. The complex Hamiltonian matrix $H(\eta)$ is diagonalized for a number of η values to obtain the resonance energy. The η trajectories are examined by using logarithmic velocity $\eta \frac{\delta E}{\delta \eta}$. To determine the optimal CAP strength (η_{opt}), one can employ the condition $\eta \frac{\delta E}{\delta \eta} = \min$[18].

One can also determine the optimal CAP strength by graphically analyzing the η-trajectory, as at the optimum, the resonance is associated with a stabilization point or cusp. To optimize the box size, several calculations are performed at the optimal η value. The chosen optimized box size is the one where the resonance energies show minimal variation.
Resonance Energy is defined as

$$E_{res} = E_{anion} - E_{neutral} \tag{4}$$

3 Self-Consistent-Field Method

The method used in this work is a modified version of SCF after removing the states. Initially, usual SCF calculation is carried out for neutral species and then the identification of the valence antibonding orbital state that is going to be filled by the extra electron. Understanding

the definition of the valence antibonding orbital is crucial since the choice of valence antibonding orbital state is a significant step in the process. The valence antibonding orbital refers to the state in which an additional electron will occupy and is the state that is most stabilized at a higher nuclear charge. To accurately identify the valence antibonding orbital, a methodology that combines the nuclear charge stabilization method with Parametric Equations of Motion (PEM) is employed, as discussed in previous articles[50, 51]. When using a heavily diffuse basis set, it is possible to encounter states with the same symmetry as valence antibonding orbital. This can lead to avoided crossings in the charge stabilization plot due to the mixing of states, which complicates the identification of the valence antibonding orbital. To effectively address these avoided crossings, a modified PEM alongside the charge stabilization method is implemented. This approach leads to a precise identification of the valence antibonding orbital[51]. All the notations are taken from Szabo[56] and carry same meaning until mentioned explicitly. Following the conventional SCF, after diagonalizing the F' , the orbital energies(ϵ) and C' is obtained,

$$F'C' = C'\epsilon \tag{5}$$

,

where F' is defined conventionally as

$$F' = X^T F X, \tag{6}$$

X is canonical orthogonalizing transformation matrix[56] which is defined as

$$X = U s^{-\frac{1}{2}} \tag{7}$$

and matrix elements corresponding to Fock-matrix are;

$$F_{mn} = T_{mn} + V_{mn}^{nucleus} + \sum_{\lambda\sigma} P_{\lambda\sigma}[(mn|\sigma\lambda) - \frac{1}{2}(m\lambda|\sigma n)] \tag{8}$$

where

$$P_{\lambda\sigma} = \sum_{a}^{occ} C_{\lambda a} C_{\sigma a}^{\star}, \tag{9}$$

and T_{mn} is the matrix elements of kinetic energy whereas $V_{mn}^{nucleus}$ is the matrix elements of the electron-nucleus attraction corresponds to all nuclei.

The second step involves the reduction of states which are not important. After identifying the valence antibonding orbital, remove the states located between the HOMO and the valence antibonding orbital from the C' matrix. The matrix obtained after the removal of states is now referred to as C'_{red} and from the obtained C'_{red} matrix , C_{red} matrix is prepared as

$$C_{red} = X C'_{red}. \tag{10}$$

This obtained C_{red} from the SCF calculation on the neutral molecule serves as the initial guess for the desired species, i.e., for anions or excited states. Using C_{red}, the new Fock-matrix is evaluated for the desired system by modifying the occupation number.

And then F'_{red} matrix is generated as

$$F'_{red} = X^T F_{red} X \tag{11}$$

Performing the following transformation on F'_{red} gives;

$$F'' = U^T F'_{red} U \tag{12}$$

where $U = C'_{red}$ and the dimension of F'' decreases by the number of states removed compared to the dimension of F matrix.

The obtained F$''$ is then solved for the following eigen-value problem

$$F'' C'' = C'' \epsilon'' \tag{13}$$

to obtain the orbital energies of the remaining states and corresponding C''. Now the obtained C'' is used to make new C'_{red} by

$$C'_{red} = U C''. \tag{14}$$

This completes an iteration, and the obtained C'_{red} from this iteration is used to initiate the next iteration by going back to equation 10. When two consecutive iterations yield the same result i.e., convergence is achieved, the process is stopped. This scheme is followed for unrestricted calculations, as these metastable anions belong to an odd-electron species.

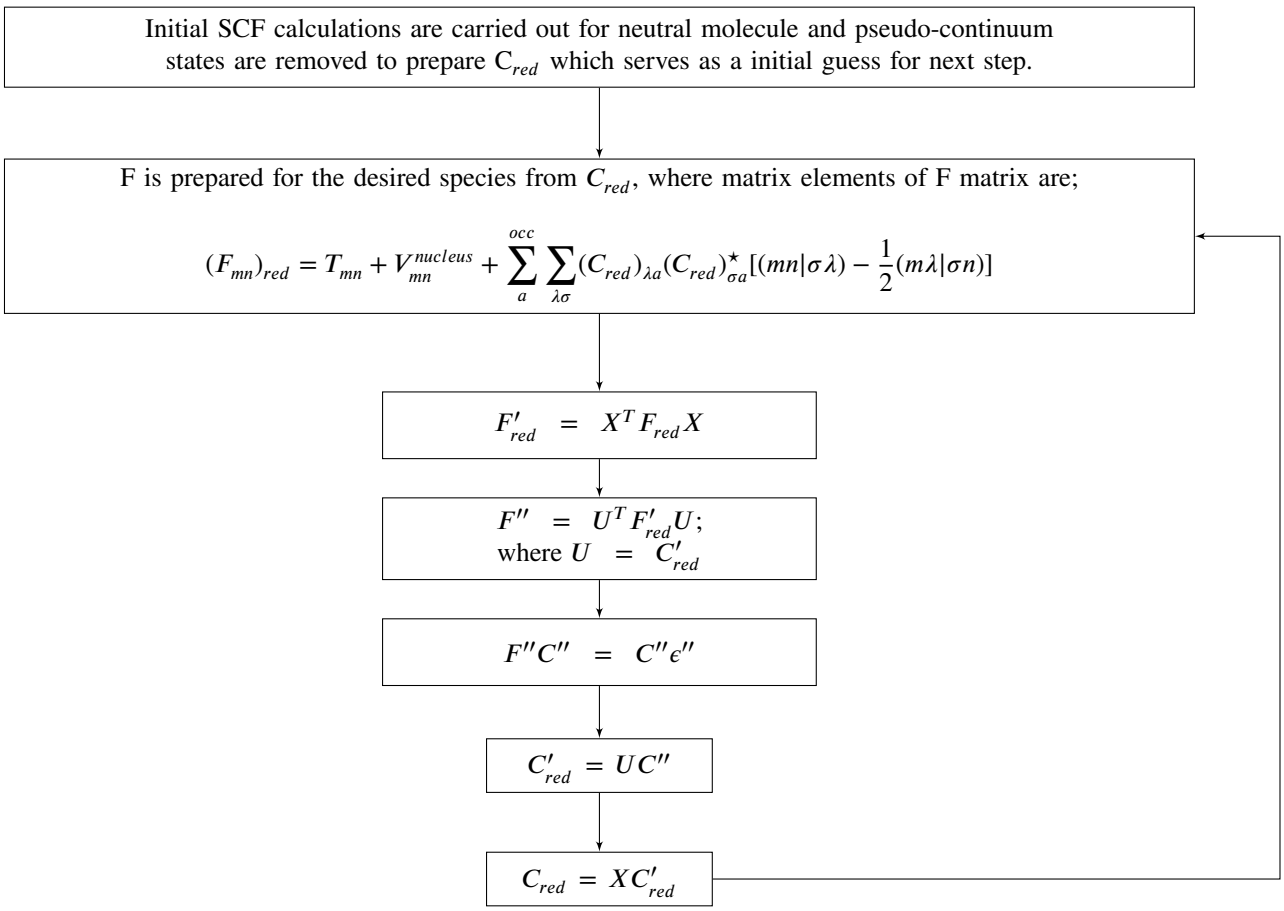


Fig. 1: Flow chart of SCF method after removing pseudo-continuum states.

4 Results and discussions

All quantum chemistry calculations are performed using the Molgw[57] package. The package is modified for the non-Hermitian calculations and for the SCF approach after removal of pseudo-continuum states. The cube files generated from MolGW are used to plot the orbitals using the Gaussian16[58] package. All calculations are performed using Cartesian Gaussian functions. To study an anionic $C_2H_4^-$ molecule and $HCHO^-$, the equilibrium geometries of a neutral C_2H_4 molecule and HCHO is utilized. The geometry parameters are provided in the Table 1 for both the molecules. The coordinates for C_2H_4 and $HCHO^-$ are provided in the Supporting Information.

4.1 Effect of removal of pseudo-continuum states on neutral ethylene (C_2H_4) and formaldehyde (HCHO) molecules

Molecule	C-C	C-H	C-O	∠HCH	∠HCC	∠HCO
C_2H_4	1.339Å	1.086Å	-	117.6°	121.2°	-
HCHO	-	1.111Å	1.205Å	116.13°	-	121.9°

Table 1: Tabular data for bond distances and bond angles for both the molecules.

This article presents an approach to obtain the meaningful SCF solution for a metastable anion by performing the SCF calculation after removing pseudo-continuum states. Before proceeding, it is essential to understand the significance of these removed pseudo-continuum states in relation to correlation energy and their impact on it. To illustrate this, an MP2 calculation is performed on a neutral molecule using various diffuse basis sets, including additional augmentations for both scenarios: one where all states are included and another where the pseudo-continuum states are removed. The nuclear charge stabilization calculations are performed using PEM to accurately identify the valence antibonding orbital. All states between HOMO and the valence antibonding orbital are excluded to perform modified SCF calculations, as these states are pseudo-continuum.

Additional s-type and p-type basis functions are included to accurately describe the resonance wavefunction. The effect of adding s-type and p-type diffuse functions on correlation energy is also observed. These augmentations are done by multiplying the smallest exponent of the previous basis set by $1/2^n$, where n is a positive integer. After performing MP2 calculations using the cc-pVTZ+nsmp basis sets, it was found that these pseudo-continuum states contribute only 1% to 2.2% and 4.3 % of the total correlation energy for C_2H_4 and HCHO respectively.

The correlation energies for both the cases are obtained, and the differences using different basis sets are reported in Table 2 for C_2H_4 and in Table 3 for HCHO. For instance, with the cc-pVTZ+8p basis set, the change in correlation energy is approximately 2.2%, with 36 states removed for C_2H_4 and the change in correlation energy is approximately 4.3%, with 33 states removed for HCHO. However, when the valence antibonding orbital is also excluded (i.e., removed along with pseudo-continuum states), the total change in correlation energy is nearly 9% and 14% C_2H_4 and HCHO respectively. This indicates that the localized state, or valence antibonding orbital, significantly affects the correlation energy. The overall difference in correlation energy when all the pseudo-continuum states between HOMO and valence antibonding orbital are removed is significantly lower than the contribution from the valence antibonding orbital alone in the correlation energy. Therefore, these pseudo-continuum states do not significantly impact the correlation energy.

Basis Set	Correlation Energy with pseudo-continuum states(in a.u.)	Correlation Energy without pseudo-continuum states(in a.u.)	Difference in Correlation Energy (in a.u.)	% Difference	Number of states removed
cc-pVTZ+3p	-0.3744	-0.3719	0.0025	0.67	6
cc-pVTZ+4p	-0.3745	-0.3697	0.0048	1.28	12
cc-pVTZ+5p	-0.3745	-0.3680	0.0065	1.73	18
cc-pVTZ+6p	-0.3745	-0.3670	0.0075	2.00	24
cc-pVTZ+7p	-0.3745	-0.3665	0.0080	2.13	30
cc-pVTZ+8p	-0.3745	-0.3663	0.0082	2.18	36
cc-pVTZ+8p	-0.3745	-0.3423	0.0322	8.59	37 (Including valence antibonding orbital)
cc-pVTZ+5s	-0.3739	-0.3708	0.0031	0.83	6
cc-pVTZ+5s8p	-0.3746	-0.3649	0.0097	2.58	40

Table 2: The table presents the correlation energy obtained using conventional SCF method, as well as the results after removing pseudo-continuum states. It also includes the differences and percentage differences, along with the number of states removed using various basis sets for neutral C_2H_4 molecule.

Basis Set	Correlation Energy with pseudo-continuum states(in a.u.)	Correlation Energy without pseudo-continuum states(in a.u.)	Difference in Correlation Energy (in a.u.)	% Difference	Number of states removed
cc-pVTZ+3p	-0.4255	-0.4233	0.0022	0.51	3
cc-pVTZ+4p	-0.4255	-0.4184	0.0071	1.67	9
cc-pVTZ+5p	-0.4256	-0.4140	0.0115	2.70	15
cc-pVTZ+6p	-0.4256	-0.4103	0.0153	3.59	21
cc-pVTZ+7p	-0.4256	-0.4080	0.0175	4.11	27
cc-pVTZ+8p	-0.4256	-0.4071	0.0185	4.34	33
cc-pVTZ+8p	-0.4256	-0.3693	0.0563	13.22	34 (Including valence antibonding orbital)
cc-pVTZ+5s	-0.4249	-0.4223	0.0025	0.59	5
cc-pVTZ+5s8p	-0.4265	-0.4070	0.0194	4.54	36

Table 3: The table presents the correlation energy obtained using conventional SCF method, as well as the results after removing pseudo-continuum states. It also includes the differences and percentage differences, along with the number of states removed using various basis sets for neutral HCHO molecule.

It is also important to note that the computational time remains nearly the same regardless of how many diffuse functions are added compared to the basis set without these additional functions. This is because all the diffuse states that lie between the HOMO and the valence antibonding orbital are excluded from the calculations. Remaining states can now be employed to study metastable anions and excited states, as these pseudo-continuum states do not significantly affect the correlation energy. Regarding the time taken for calculations: once the states are removed, the calculations will naturally become faster. For comparison, we have reported the calculation times for the neutral C_2H_4 molecule with all states included versus the times taken after the removal of pseudo-continuum states for the cc-pVTZ+7p/8p basis set. Data for CPU time taken with all the states and after removing pseudo-continuum states using cc-pVTZ+7p/8p basis sets for C_2H_4 is provided in supporting information.

4.2 Ethylene anion ($C_2H_4^-$) and Formaldehyde anion ($HCHO^-$)

The electron-attached states of metastable anions are associated with a finite lifetime, and, their wavefunctions are not square-integrable. To address this issue and make the wavefunction square-integrable, the Complex Absorbing Potential (CAP) is added to the Fock-matrix in this

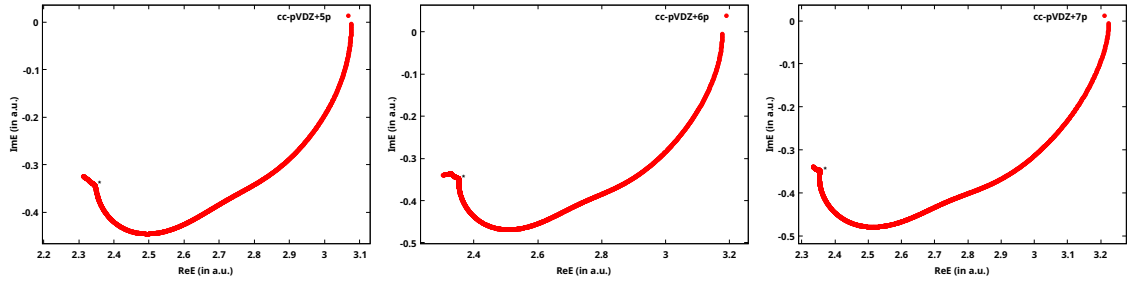
article. Additionally, the lifetime corresponding to the electron-attached state is also achieved. CAP has been applied on the both neutral and anionic species. The optimized box size is chosen from the ref[38] where box size is optimized for ethylene and formaldegyde anion. The optimal box size for the both molecules are included in supporting information.

The calculation for metastable anion to obtain the η trajectory is carried out in two steps:
i) For each η, neutral molecule self-consistent field (SCF) calculations are performed, and the valence antibonding orbital is identified.
ii) An SCF calculation is carried out for anions by modifying the occupation number (i.e., by adding an extra electron in valence antibonding orbital state) after removing all states between the HOMO and the valence antibonding orbital.

An important concern arises regarding the accuracy of the SCF solution obtained for the metastable anion after removing the pseudo-continuum states. The conventional SCF calculations for the metastable anion at a specific η value show reasonable results, suggesting that the singly occupied molecular orbital (SOMO) has a localized $\pi^\star$ character for the C_2H_4 anion at that specific η value (i.e., no pseudo-continuum states between SOMO and SOMO-1 exist). This indicates that the extra electron occupies the correct orbital, rather than a diffuse orbital, which means that variational collapse is not occurring for metastable anion. Therefore, the conventional SCF solution at this η value is considered the standard solution for the metastable anion, serving as a basis for comparison with results from calculations where pseudo-continuum states are removed. The procedure described above is followed to obtain the SCF solution for a metastable anion after removing the pseudo-continuum states from the solution for a neutral molecule. Remarkably, it is found that both solutions are identical. At this particular η, MP2-level energies are also obtained for anionic and neutral species in both the cases(i.e., with all the states and with after the removal of pseudo-continuum states), which are provided in Supporting Information.

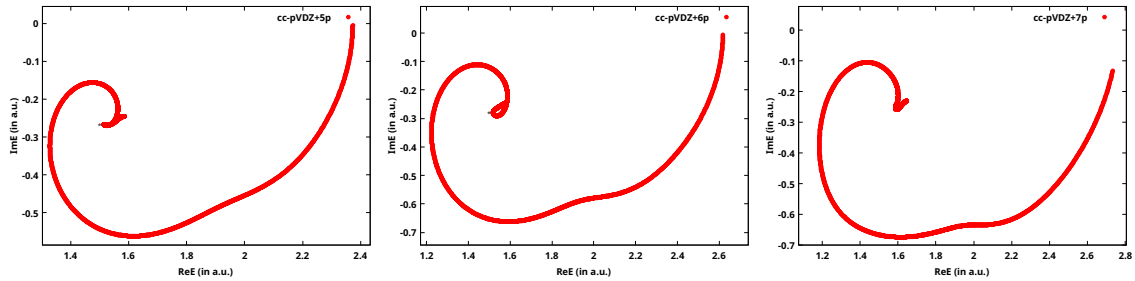
It is worth noting that there may be rearrangements of states occurring in step one, which means that the position of the valence antibonding orbital at two different η values from the HF calculation might not be the same. This makes it extremely challenging to keep track of the orbital numbers between the HOMO and the valence antibonding orbital, as it requires significant human effort to manage. An alternative solution to this problem is to implement the PEM-CAP[59] approach in this step, which simplifies the process of tracking orbitals. With this method, one can easily identify and remove the appropriate number of states at any η value. The solution obtained at the HF level is then used for post-SCF calculations (in this case, employing MP2). At the optimized the box size, the parameter η is varied through the PEM-CAP[59] approach for different basis sets, resulting in the corresponding η trajectories.

The η trajectories at MP2 level for various basis sets are illustrated in Figure 2 for C_2H_4 and in Figure 3 for HCHO. The stabilization point, or cusp, represents the resonance energy in the η trajectory plot.



(a) MP2/cc-pVDZ+5p (b) MP2/cc-pVDZ+6p (c) MP2/cc-pVDZ+7p

Fig. 2: The η-trajectories corresponding to the $^2B_{2g}$ resonance in $C_2H_4^-$ using various basis sets at MP2 level.



(a) MP2/cc-pVDZ+5p (b) MP2/cc-pVDZ+6p (c) MP2/cc-pVdZ+7p

Fig. 3: The η-trajectories corresponding to the $^2B_1$ resonance in $HCHO^-$ using various basis sets at MP2 level.

Resonance energies are obtained at MP2 level using various basis sets, as shown in Table 4 for C_2H_4 and in Table 5 for HCHO, which also includes the optimal η (η_{opt}) value. The value of S^2 was found to be in the range of 0.75–0.77 in all cases, which is close to the expected value of 0.75 for one unpaired electron.

A summary of the resonance energies, along with the experimental results and findings from earlier theoretical studies, is presented in Table 6 for C_2H_4 and in Table 7 for HCHO. The results of our theoretical calculations align well with the experimental measurements. For C_2H_4, a high-accuracy theoretical approach such as CAP-EOM-EA-CCSD predicts a resonance position of approximately 2.03 eV and a resonance width of 0.33 eV using the aug-cc-pVTZ+3s3p3d basis. In contrast, our methodology applied at the MP2 level with the aug-cc-pVTZ+5p basis yields a resonance position of 2.35 eV and a resonance width of 0.69 eV, which are quite comparable. Recent calculations using the MR-CIS method with the cc-pVTZ+3p basis indicate a resonance position of 2.504 eV and a resonance width of 0.503 eV. Other theoretical results also show reasonable agreement with our findings.

Basis Set	Resonance Energy at MP2 Level		
	Resonance Position (eV)	Resonance Width (eV)	η_{opt}
cc-pVDZ+5p	2.35	0.69	0.0041
cc-pVDZ+5s5p	2.35	0.69	0.0042
cc-pVDZ+6p	2.35	0.69	0.0041
cc-pVDZ+7p	2.35	0.69	0.0042

Table 4: Resonance energies for $^2B_{2g}$ resonance in $C_2H_4^-$ at MP2 level are presented using different basis sets.

Basis Set	Resonance Energy at MP2 Level		
	Resonance Position (eV)	Resonance Width (eV)	η_{opt}
cc-pVDZ+5p	1.51	0.53	0.0043
cc-pVDZ+5s5p	1.51	0.53	0.0046
cc-pVDZ+6p	1.52	0.55	0.0047
cc-pVDZ+7p	1.58	0.52	0.0046

Table 5: Resonance energies for $^2B_1$ resonance in $HCHO^-$ at MP2 level using different basis sets.

For HCHO, the CAP-EOM-EA-CCSD method predicts a resonance position of about 1.31 eV and a resonance width of 0.28 eV, using the aug-cc-pVTZ+3s3p3d basis. Our MP2 methodology with the cc-pVTZ+5p basis predicts a resonance position of 1.51 eV and a width of 0.53 eV. The R-matrix method predicts a resonance position of 1.46 eV and a width of 0.79 eV, which is fairly close to our results. Overall, our methodology provides a reasonable estimate of the resonance energy for HCHO and for C_2H_4.

Reference/Method	Resonance Energy(in eV)	Resonance Width(in eV)
Electron transmission[60, 61]	1.80	0.70
Complex Kohn[62]	1.83	0.46
Diagonal 2ph-TDA biorthogonal dilated electron propagator [63]	1.89	0.18
Complex Kohn[64]	1.85	0.50
ACCC[65]	1.86	0.47
Stabilization method/ EOM-CCSD/aug-cc-pVTZ+3p [43]	2.06	0.64
CAP-EOM-EA-CCSD/ aug-cc-pVTZ+3s3p3d (0th order) [38]	2.09	0.430
CAP-EOM-EA-CCSD/ aug-cc-pVTZ+3s3p3d (1st order) [38]	2.03	0.33
CAP/SAC-CI[66]	2.02	0.46
SA-15-CASSCF(3e, 20o)/cc-pVTZ+X[3p][67]	3.119	0.634
MR-CIS/SA-8-CASSCF(3e, 9o)/cc-pVTZ+[3p][67]	2.504	0.503
MR-CIS/SA-6-CASSCF(3e, 7o)/cc-pVDZ+[3p][67]	2.617	0.592
MP2/cc-pVDZ+5p (this work)	2.35	0.69

Table 6: Tabular data corresponding to previous theoretical and experimental result for resonance energy and width of the $^2B_{2g}$ resonance in in $C_2H_4^-$.

Reference/Method	Resonance Energy(in eV)	Resonance Width(in eV)
Electron transmission[60, 68]	1.0/0.86	
Vibrational excitation[69]	0.87	
Complex Kohn[70]	1.0	0.5
Diagonal 2ph-TDA[71]	0.89	0.12
R-matrix method/DZPd[72]	1.46	0.79
CAP/EOM-EA-CCSD (1st order)[38]	1.31	0.28
CAP/SAC-CI[66]	1.18	0.38
EOM-EA-CCSD[73]	1.16	0.57
CAP/XMS-CASPT2[74]	1.27–1.28	0.47–0.48
SA-15-CASSCF(3e, 16o)/cc-pVTZ+X[4p][67]	2.43	0.34
SA-19-CASSCF(3e, 20o)/cc-pVTZ+X[2s5p2d][67]	2.633	0.416
MR-CIS/SA-7-CASSCF(3e, 8o)/cc-pVDZ+[3p] [67]	0.931	0.211
MP2/cc-pVDZ+5p (this work)	1.51	0.53

Table 7: Tabular data corresponding to previous theoretical and experimental result for resonance Energy and width of the $^2B_1$ resonance of $HCHO^-$.

5 Conclusion

This article provides a meaningful SCF solution for metastable anions after removing the pseudo-continuum states by modifying the Fock matrix. CAP is implemented at the HF-level to make the metastable anion wavefunction square integrable, and to obtain the lifetime of the attached electron. The obtained SCF solution can then be used for post-SCF calculations, such as Configuration Interaction (CI), Coupled Cluster Singles and Doubles (CCSD), Møller-Plesset perturbation theory (MP2), and MP4, to account for electron correlation. In the present case, MP2 calculations are performed on C_2H_4 and HCHO molecules, and it is shown that

removing these pseudo-continuum states has no significant effect on the correlation energy. This method is extremely important as no variational collapse will occur for the metastable anion if the electronic state filled by the extra electron is identified correctly. Additionally, it significantly reduces computational time, making it a cost-effective approach for studying species that require diffuse functions to accurately describe the system. Two anionic species have been studied using this method, and their resonance energies are found to be in decent agreement with previously available theoretical and experimental results. This method could potentially be expanded to investigate core-excited shape or Feshbach resonances in the future. However, this article currently focuses only on shape resonances.

6 Acknowledgments

The authors would like to acknowledge the PARAM-ISHAN and PARAM-KAMRUPA supercomputing centers in IIT Guwahati for providing us with high-performance computing facilities. Deepak Kumar is thankful to the Ministry of Education, India, and IIT Guwahati for the research fellowship.

7 Statement and Declaration

The authors declare no competing interests.

References

[1] Simons, J.; Jordan, K. D. Ab initio electronic structure of anions. *Chem. Rev.* **1987**, *87*, 535–555.

[2] Jordan, K. D.; Burrow, P. D. Temporary anion states of polyatomic hydrocarbons. *Chem. Rev.* **1987**, *87*, 557–588.

[3] Simons, J. Molecular anions. *J. Phys. Chem. A* **2008**, *112*, 6401–6511.

[4] Ehara, M.; Sommerfeld, T. CAP/SAC-CI method for calculating resonance states of metastable anions. *Chem. Phys. Lett.* **2012**, *537*, 107–112.

[5] Gayvert, J. R.; Bravaya, K. B. Application of box and Voronoi CAPs for metastable electronic states in molecular clusters. *J. Phys. Chem. A* **2022**, *126*, 5070–5078.

[6] Jagau, T.-C. Theory of electronic resonances: fundamental aspects and recent advances. *Chem. Comm.* **2022**, *58*, 5205–5224.

[7] Simons, J. Molecular Anions Perspective. *J. Phys. Chem. A* **2023**, *127*, 3940–3957.

[8] Ghosh, A.; Vaval, N.; Pal, S. Equation-of-motion coupled-cluster method for the study of shape resonance. *The Journal of Chemical Physics* **2012**, *136*.

[9] Bravaya, K. B.; Zuev, D.; Epifanovsky, E.; Krylov, A. I. Complex-scaled equation-of-motion coupled-cluster method with single and double substitutions for autoionizing excited states: Theory, implementation, and examples. *The Journal of chemical physics* **2013**, *138*.

[10] Benda, Z.; Jagau, T.-C. Communication: Analytic gradients for the complex absorbing potential equation-of-motion coupled-cluster method. *The Journal of chemical physics* **2017**, *146*.

[11] Aguilar, J.; Combes, J.-M. A class of analytic perturbations for one-body Schrödinger Hamiltonians. *Commun. Math. Phys.* **1971**, *22*, 269–279.

[12] Balslev, E.; Combes, J.-M. Spectral properties of many-body Schrödinger operators with dilatation-analytic interactions. *Commun. Math. Phys.* **1971**, *22*, 280–294.

[13] Chuljian, D. T.; Simons, J. Coordinate rotation studies of H^-, He^-, Be^-, Mg^- resonances: Basis set and configuration list dependence. *Int. J. Quantum Chem.* **1983**, *23*, 1723–1738.

[14] Moiseyev, N.; Hirschfelder, J. Representation of several complex coordinate methods by similarity transformation operators. *J. Chem. Phys.* **1988**, *88*, 1063–1065.

[15] Kalita, D. J.; Gupta, A. K. Use of modified smooth exterior scaling method as an absorbing potential and its application. *J. Chem. Phys.* **2011**, *134*.

[16] Banuary, M.; Gupta, A. K. Application of Modified Smooth Exterior Scaling Method to Study $^2\Pi_g$ N_2^- and $^2\Pi$ CO^- Shape Resonances. *ACS omega* **2023**, *8*, 7143–7150.

[17] Banuary, M.; Kumar, D.; Gupta, A. K. Use of the dilated electron propagator in conjunction with the modified smooth exterior scaling method to characterize ^2S $Be^+(1s^{-1})$, ^2S $Ne^+(1s^{-1})$ Auger and ^2P Be^- shape resonances. *New J. Chem.* **2024**, *48*, 4772–4782.

[18] Riss, U.; Meyer, H.-D. Calculation of resonance energies and widths using the complex absorbing potential method. *J. Phys. B: At. Mol. Opt. Phys.* **1993**, *26*, 4503.

[19] Jolicard, G.; Austin, E. J. Optical potential method of calculating resonance energies and widths. *Chem. Phys.* **1986**, *103*, 295–302.

[20] Jolicard, G.; Austin, E. J. Optical potential stabilisation method for predicting resonance levels. *Chem. Phys. Lett.* **1985**, *121*, 106–110.

[21] Tozer, D. J.; De Proft, F. Modeling temporary anions in density functional theory: Calculation of the Fukui function. *J. Chem. Phys.* **2007**, *127*.

[22] Sablon, N.; De Proft, F.; Geerlings, P.; Tozer, D. J. On the position of the potential wall in DFT temporary anion calculations. *Phys. Chem. Chem. Phys.* **2007**, *9*, 5880–5884.

[23] Taylor, H. S. Models, interpretations, and calculations concerning resonant electron scattering processes in atoms and molecules. *Adv. Chem. Phys.* **1970**, 91–147.

[24] Hazi, A. U.; Taylor, H. S. Stabilization method of calculating resonance energies: Model problem. *Phys. Rev. A* **1970**, *1*, 1109.

[25] Simons, J. Resonance state lifetimes from stabilization graphs. *J. Chem. Phys.* **1981**, *75*, 2465–2467.

[26] Lauderdale, J. G.; Truhlar, D. G. Stabilization calculations of resonance energies for the coplanar reactions H+FH and $H+H_2$. *J. Chem. Phys.* **1986**, *84*, 192–196.

[27] Macías, A.; Riera, A. Stabilization versus feshbach techniques in the determination of resonances. *Chem. Phys. Lett.* **1987**, *139*, 300–305.

[28] Macias, A.; Riera, A. On calculations of resonance parameters from stabilization graphs. *J. Chem. Phys.* **1992**, *96*, 2877–2880.

[29] Simons, J. Analysis of Stabilization and Extrapolation Methods for Determining Energies and Lifetimes of Metastable Electronic States. *J. Phys. Chem. A* **2021**, *125*, 7735–7749.

[30] Nestmann, B.; Peyerimhoff, S. Calculation of the discrete component of resonance states in negative ions by variation of nuclear charges. *J. Phys. B: At. Mol. Phys.* **1985**, *18*, 615.

[31] Nestmann, B.; Peyerimhoff, S. CI method for determining the location and width of resonances in electron-molecule collision processes. *J. Phys. B: At. Mol. Phys.* **1985**, *18*, 4309.

[32] Sommerfeld, T.; Riss, U.; Meyer, H.; Cederbaum, L.; Engels, B.; Suter, H. Temporary anions-calculation of energy and lifetime by absorbing potentials: The resonance. *J. Phys. B: At. Mol. Opt. Phys.* **1998**, *31*, 4107.

[33] Anusiewicz, I.; Skurski, P. Shape resonance of the ethylene anion stabilized in a molecular trap. *Chem. Phys. Lett.* **2003**, *370*, 345–352.

[34] Feuerbacher, S.; Sommerfeld, T.; Cederbaum, L. S. Extrapolating bound state data of anions into the metastable domain. *J. Chem. Phys.* **2004**, *121*, 6628–6633.

[35] Sommerfeld, T.; Ehara, M. Short-range stabilizing potential for computing energies and lifetimes of temporary anions with extrapolation methods. *J. Chem. Phys.* **2015**, *142*.

[36] Bacic, Z.; Simons, J. Resonance energies and lifetimes from stabilization-based methods. *J. Phys. Chem.* **1982**, *86*, 1192–1200.

[37] Whitehead, A.; Barrios, R.; Simons, J. Stabilization calculation of the energy and lifetime of metastable SO_4^{2-}. *J. Chem. Phys.* **2002**, *116*, 2848–2851.

[38] Zuev, D.; Jagau, T.-C.; Bravaya, K. B.; Epifanovsky, E.; Shao, Y.; Sundstrom, E.; Head-Gordon, M.; Krylov, A. I. Complex absorbing potentials within EOM-CC family of methods: Theory, implementation, and benchmarks. *J. Chem. Phys.* **2014**, *141*.

[39] Landau, A.; Moiseyev, N. Molecular resonances by removing complex absorbing potentials via Padé; Application to CO^- and N_2^-. *The Journal of Chemical Physics* **2016**, *145*.

[40] Fujimoto, M. M.; de Lima, E. V.; Tennyson, J. Elastic scattering of low-energy electrons by CH_3CN and CH_3NC molecules. *The European Physical Journal D* **2015**, *69*, 153.

[41] Cheng, H.-Y.; Chen, C.-W.; Chang, J.-T.; Shih, C.-C. Application of the stabilization method to temporary anion states of CH_3CN, CH_3NC, CH_3SCN, and CH_3NCS in density functional theory with asymptotically corrected potentials. *The Journal of Physical Chemistry A* **2011**, *115*, 84–93.

[42] Falcetta, M.; Jordan, K. D. Assignments of the temporary anion states of the chloromethanes. *Journal of Physical Chemistry* **1990**, *94*, 5666–5669.

[43] Falcetta, M. F.; DiFalco, L. A.; Ackerman, D. S.; Barlow, J. C.; Jordan, K. D. Assessment of various electronic structure methods for characterizing temporary anion states: Application to the ground state anions of N_2, C_2H_2, C_2H_4, and C_6H_6. *J. Phys. Chem. A* **2014**, *118*, 7489–7497.

[44] Falcetta, M.; Jordan, K. Ab initio investigation of the temporary anion states of silane and the linear silanes:(Si_nH_{2n+2}), n= 2-5. *Chemical physics letters* **1999**, *300*, 588–594.

[45] Rajbongshi, H.; Kumar, D.; Banuary, M.; Gupta, A. K. *The Journal of Physical Chemistry A*, submitted.

[46] Cheng, H.-Y.; Chen, C.-W. Energy and lifetime of temporary anion states of uracil by stabilization method. *The Journal of Physical Chemistry A* **2011**, *115*, 10113–10121.

[47] Fennimore, M. A.; Matsika, S. Core-excited and shape resonances of uracil. *Physical Chemistry Chemical Physics* **2016**, *18*, 30536–30545.

[48] Bouskila, G.; Landau, A.; Haritan, I.; Moiseyev, N.; Bhattacharya, D. Complex energies and transition dipoles for shape-type resonances of uracil anion from stabilization curves via Padé. *The Journal of Chemical Physics* **2022**, *156*.

[49] Kumar, D.; Gupta, A. K. Self-consistent-field solution for unstable anions. *Phys. Rev. A* **2024**, *110*, 062821.

[50] Kumar, D.; Banuary, M.; Gupta, A. K. An Innovative Approach for Precise Identification of the Lowest Unoccupied Molecular Orbital Using the Parametric Equation of Motion. *J. Chem. Theory Comput.* **2024**, *20*, 6009–6019.

[51] Kumar, D.; Gupta, A. K. A unique approach to address avoided crossings in the charge stabilization curve for LUMO identification. *J. Chem. Phys.* **2024**, *161*.

[52] Dora, A.; Tennyson, J.; Bryjko, L.; Van Mourik, T. R-matrix calculation of low-energy electron collisions with uracil. *The Journal of chemical physics* **2009**, *130*.

[53] Jagau, T.-C. Non-iterative triple excitations in equation-of-motion coupled-cluster theory for electron attachment with applications to bound and temporary anions. *The Journal of chemical physics* **2018**, *148*.

[54] Thodika, M.; Matsika, S. Projected complex absorbing potential multireference configuration interaction approach for shape and Feshbach resonances. *Journal of Chemical Theory and Computation* **2022**, *18*, 3377–3390.

[55] Santra, R.; Cederbaum, L. S.; Meyer, H.-D. Electronic decay of molecular clusters: non-stationary states computed by standard quantum chemistry methods. *Chemical physics letters* **1999**, *303*, 413–419.

[56] Szabo, A.; Ostlund, N. S. *Modern quantum chemistry: introduction to advanced electronic structure theory*; Courier Corporation, 2012.

[57] Bruneval, F.; Rangel, T.; Hamed, S. M.; Shao, M.; Yang, C.; Neaton, J. B. molgw 1: Many-body perturbation theory software for atoms, molecules, and clusters. *Comput. Phys. Commun.* **2016**, *208*, 149–161.

[58] Frisch, M. e.; Trucks, G.; Schlegel, H. B.; Scuseria, G.; Robb, M.; Cheeseman, J.; Scalmani, G.; Barone, V.; Petersson, G.; Nakatsuji, H.; others Gaussian 16. 2016.

[59] Kumar, D.; Gupta, A. K. Application of parametric equations of motion to study uracil anion. *J. Chem. Phys.* **2025**, *163*.

[60] Burrow, P.; Michejda, J. Electron transmission study of the formaldehyde electron affinity. *Chem. Phys. Lett.* **1976**, *42*, 223–226.

[61] Walker, I. C.; Stamatovic, A.; Wong, S. Vibrational excitation of ethylene by electron impact: 1–11 eV. *J. Chem. Phys.* **1978**, *69*, 5532–5537.

[62] Schneider, B. I.; Rescigno, T. N.; Lengsfield III, B.; McCurdy, C. Accurate ab initio treatment of low-energy electron collisions with ethylene. *Phys. Rev. Lett.* **1991**, *66*, 2728.

[63] Medikeri, M. N.; Mishra, M. K. Characterization of molecular shape resonances using different decouplings of the dilated electron propagator with application to $^2\Pi$ CO^- and $^2B_{2g}$ $C_2H_4{}^-$ shape resonances. *J. Chem. Phys.* **1995**, *103*, 676–682.

[64] Trevisan, C. S.; Orel, A. E.; Rescigno, T. N. Ab initio study of low-energy electron collisions with ethylene. *Phys. Rev. A* **2003**, *68*, 062707.

[65] Horacek, J.; Paidarová, I.; Curik, R. Determination of the resonance energy and width of the $^2B_{2g}$ shape resonance of ethylene with the method of analytical continuation in the coupling constant. *J. Phys. Chem. A* **2014**, *118*, 6536–6541.

[66] Sommerfeld, T.; Melugin, J. B.; Hamal, P.; Ehara, M. Resonance energies and lifetimes from the analytic continuation of the coupling constant method: Robust algorithms and a critical analysis. *J. Chem. Theory Comput.* **2017**, *13*, 2550–2560.

[67] Mondal, S.; Bravaya, K. B. Analytic Nuclear Gradients for Complex Potential Energy Surfaces: A Projected CAP Approach. *J. Chem. Theory Comput.* **2025**,

[68] Van Veen, E.; Van Dijk, W.; Brongersma, H. Low-energy electron-impact excitation spectra of formaldehyde, acetaldehyde and acetone. *Chem. Phys.* **1976**, *16*, 337–345.

[69] Benoit, C.; Abouaf, R. Low-energy electron collisions with formaldehyde: interference phenomena in the differential vibrational excitation cross section. *Chem. Phys. Lett.* **1986**, *123*, 134–138.

[70] Schneider, B. I.; Rescigno, T. N.; McCurdy, C. Resonant vibrational excitation of H_2CO by low-energy electron impact. *Phys. Rev. A* **1990**, *42*, 3132.

[71] Mahalakshmi, S.; Mishra, M. K. The $^2B_1$ shape resonance in electron-formaldehyde scattering: an investigation using the dilated electron propagator method. *Chem. Phys. Lett.* **1998**, *296*, 43–50.

[72] Vinodkumar, M.; Bhutadia, H.; Antony, B.; Mason, N. Electron-impact rotationally elastic total cross sections for H_2CO and HCOOH over a wide range of incident energy (0.01–2000 eV). *Phys. Rev. A* **2011**, *84*, 052701.

[73] White, A. F.; Epifanovsky, E.; McCurdy, C. W.; Head-Gordon, M. Second order Møller-Plesset and coupled cluster singles and doubles methods with complex basis functions for resonances in electron-molecule scattering. *J. Chem. Phys.* **2017**, *146*.

[74] Phung, Q. M.; Komori, Y.; Yanai, T.; Sommerfeld, T.; Ehara, M. Combination of a Voronoi-type complex absorbing potential with the XMS-CASPT2 method and pilot applications. *J. Chem. Theory Comput.* **2020**, *16*, 2606–2616.

Supplementary Files

This is a list of supplementary files associated with this preprint. Click to download.

- suppstates.pdf